ADVANCES IN FLOW DISPLACEMENT IMMUNOASSAY DESIGN

David Holt[1], Sina Y. Rabbany[2], Anne W. Kusterbeck[1*], Frances S. Ligler[1]

[1]*The Center for Bio/Molecular Science and Engineering, Naval Research Laboratory, Washington, D.C. 20375*

[2]*Bioengineering Program, Hofstra University, Hempstead, N.Y. 11549*

TABLE OF CONTENTS

Introduction 108
Fluid Dynamics and Mass Transport Considerations 110
Kinetics Considerations in the Displacement Immunosensor 116
Dissociation Kinetics 117
Additional Kinetics Considerations 118
Flow Displacement Immunoassay Performance 119
A. Bead Assay 119
B. Membrane Assay 124
C. Capillary Assay 126
D. Discussion 127
Applications 128
Conclusion 129

ABSTRACT

Flow immunosensors and assays based on **displacement** reactions have emerged as viable alternatives to other immunological methods such as competitive or sandwich assays. Displacement assays differ fundamentally from these standard techniques in that the observed response depends more upon **dissociation** kinetics rather than **association** kinetics. A review of the development and application of displacement immunosensors is given herein. The text is organized according to the three types of solid support matrices which have been used: bead-packed columns, membranes, and unrestricted

* To whom correspondence should be addressed.

microcapillary tubes. Since these assays are performed under flow conditions, a brief overview of relevant fluid dynamics and mass transport considerations is provided prior to the discussion of the flow immunosensors.

INTRODUCTION

Traditional immunoassays, whether direct binding[1] or competitive[2] assay formats, measure the binding of antigen to antibody and are dependent upon the **association** kinetics of the antibody-antigen reaction. However, the displacement immunoassay[3] measures the **dissociation** of a labeled antigen from immobilized antibody in the presence of unlabeled antigen under flow conditions. Flow immunosensors provide numerous benefits compared to other immunosensor formats: fast response time and short total assay time, simplicity, and portability. Unlike equilibrium-based immunoassays (e.g. ELISA), this configuration does not require incubation and washing steps or the introduction of the indicator reagents following sample loading[4]. Most importantly, many samples can be rapidly analyzed using a single aliquot of immobilized antibody.

The basic procedure for preparing and utilizing a flow displacement sensor is outlined in Figure 1. Monoclonal antibodies are immobilized onto a solid support, usually through covalent attachment. The antibody binding sites are saturated with fluorescently-labeled antigens and placed in a buffer flow stream. When unlabeled antigen is introduced, it displaces the fluorescent antigen and releases it into the flow stream. As the stream passes through a fluerometer, a signal is generated. Introduction of a positive sample induces a rapid displacement reaction which is not predicted by classical concepts describing antibody-antigen interactions in solution under equilibrium conditions.

Contrary to the functionally irreversible binding that occurs in ELISA-type systems, the displacement occurs within seconds of exposure to unlabeled antigen[5]. Several factors known to influence antibody binding were investigated in detail including flow rate[4] and antibody density[6]. Standard curves using known concentrations of unlabeled antigen can be established, and unknown concentrations can be quantified. In addition, displacement efficiency for each antigen-antibody pair can be established by the use of known antigen concentrations.

Over the years, the flow immunosensor has used three geometrically distinct support matrices for the immobilization of antibodies. The first system investigated was a column packed with porous beads[7]. Initially, the antibody was

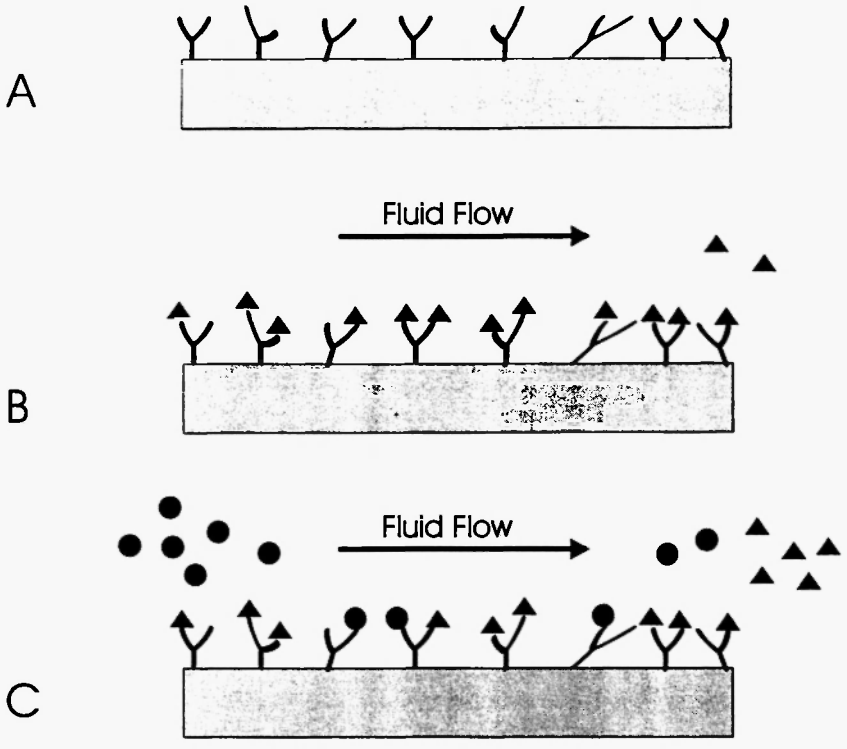

Fig. 1: Schematic representation of immobilized antibody-antigen interaction in the flow immunoassay. (a) Antibodies are immobilized via cross-linking onto the solid support. (b) The antibody binding sites are saturated with fluorophore-labeled antigens. Then buffer flow is initiated which washes off non-specifically bound labeled-antigen (not indicated) and establishes a slowly but continually decreasing fluorescence background from the spontaneous dissociation of labeled-antigen from the surface bound antibody. (c) The reagent to be detected is introduced into the buffer stream over the assay. The incoming analyte displaces the bound labeled-antigens, rendering a signal measured by a fluerometer downstream.

coupled to tresyl chloride-activated Sepharose 4B beads. Columns containing other types of porous beads such as control pore glass (CPG) and Emphaze (3M) beads were also employed. The second configuration utilized a porous, nylon membrane (Immunodyne ABC, Pall Corp., Port Washington, New York)

modified to incorporate surface reactive sites for covalent attachment of antibodies and other proteins[8]. The third and most recent design utilized glass micro-capillary tubes as the solid support. The microcapillaries were silanized to immobilize the antibody via a heterobifunctional cross-linking agent[9].

FLUID DYNAMICS AND MASS TRANSPORT CONSIDERATIONS

The three solid supports present different fluid dynamic and mass transfer conditions which must be considered when designing and using a flow immunoassay system. Therefore a cursory review of basic fluid dynamic principles is useful. In an *unrestricted* microcapillary, the bulk movement of fluid (convection) occurs in only one direction (parallel to the axis of the conduit) since the flow generally is not turbulent*. A fully developed, laminar flow in a circular tube has a parabolic velocity profile as shown in Figure 2. This is the well known Hagen-Poiseuille flow condition[10] which is described by Equations (1) and (2)

$$v(r) = v_{max}\left(1 - \frac{r^2}{R^2}\right) \tag{1}$$

$$v_{max} = \frac{\Delta p R^2}{4 \mu L} \tag{2}$$

where Δ p is the pressure difference between the entrance and exit, μ is the fluid viscosity, and R and L are the radius and length of the reactor, respectively. At the center of the tube, the fluid velocity is at a maximum and decreases (in proportion to the square of the distance from the center) to zero at the wall (no slip condition). The magnitude of the maximum velocity is proportional to the square of the radius. Therefore, given a constant pressure gradient, the velocity (and flow rate) increase as the bore radius increases. However, the flow rate, given by Equation (3), is typically held constant in practical experiments. For a

* For typical flow rates used in the experiments reviewed herein, the Reynolds numbers (Re, ratio of inertial to viscous forces) are not greater than ten. Turbulent flows are characterized by Re greater than 2000 for flows in unobstructed, closed channels. See Reference 10.

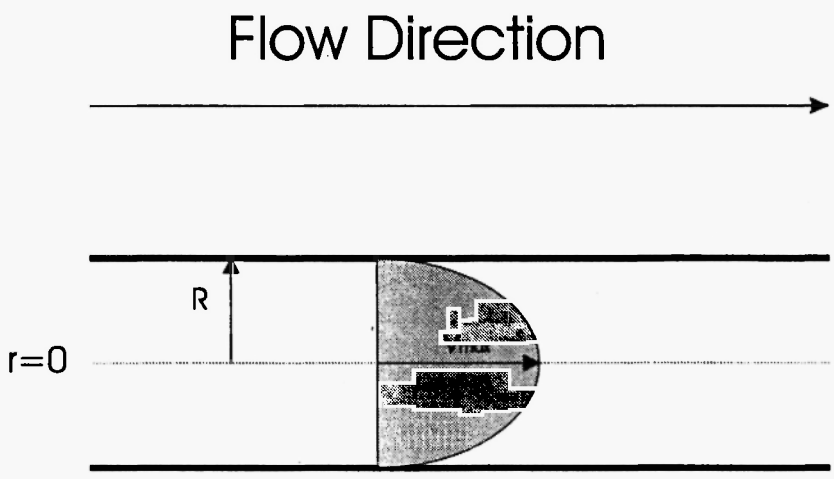

Fig. 2: Fluid velocity profile of a fully developed, steady laminar flow in a circular or rectangular channel.

constant flow rate to be maintained, the flow velocity and consequently the pressure gradient must increase as the radius of the reactor decreases.

$$Q = \frac{\pi R^4 \Delta p}{8 \mu L} \tag{3}$$

The parabolic velocity profile impacts the sensitivity of sensors in which the convection of material occurs by laminar flow. Peak broadening occurs because material in the center of the channel travels faster than material near the walls[11]. The magnitude of this axial dispersion increases with the length of the channel and flow rates. Thus, to maximize the sensitivity, an optimum balance between the time period allowed for reaction and the dispersive effects of laminar flow is needed.

In a capillary-based system, some analyte will be present initially in the molecular-scale fluid layer adjacent to the surface. However, once this supply is depleted, the mass transport process responsible for getting analyte to the reactor wall is diffusion perpendicular to the flow direction. This is particularly true when the volume of sample injected is less than or equal to the reactor volume. Convection of analyte to the reaction surface is not a factor since the flow in a capillary is not turbulent. Thus, a capillary-based sensor cannot be considered a one-dimensional device even though fluid flow occurs in only one

direction. Accordingly, performance is dependent upon the balance between the displacement reaction kinetics, diffusion of the analyte to the surface, and convection through the system.

An understanding of the balance between analyte transport through a capillary via convection and transport to the reaction surface by diffusion can be gained with a few straightforward algebraic manipulations. From elementary diffusion theory (Fick's Laws), an estimation for the effective distance (r_{eff}) over which a substance of diffusivity D diffuses in time t is given by

$$r_{eff} = \gamma(D\,t)^{1/2} \tag{4}$$

where γ is a geometrical parameter. For a capillary of length L and radius R, and a flow rate Q through the capillary, the average residence time in the system is

$$t = \pi R^2 L / Q \tag{5}$$

i.e. the volume divided by the flow rate. Substituting (5) into (4) yields

$$r_{eff} = \gamma\, R\, (\pi\, D\, L / Q)^{1/2} \tag{6}$$

Further rearrangement gives an expression which is independent of the radius or diameter of the capillary

$$r_{eff} / R = \gamma\, (\pi\, D\, L / Q)^{1/2} \tag{7}$$

This expression may be interpreted as the fraction of the capillary radius that can be traversed by the diffusing analyte while it is in residence. The ratio Q/LD is a Peclet number, a dimensionless quantity common to chemical engineering which describes the relative contributions of convective and diffusive mass transport processes[12]. If one makes the relatively safe assumption that the system sensitivity is some function of this ratio, then longer capillaries and/or slower flow rates should yield greater displacement responses. This is an intuitive result which has been verified experimentally (as will be shown). An additional implication of radial diffusion is that it acts to blunt the parabolic velocity profile[11]. This reduces the extent of axial dispersion (peak broadening) caused by the laminar flow conditions (material in the center of the capillary traveling faster than material near the walls). This is another argument for reducing the flow velocity.

For flow in porous media, additional fluid dynamic complications arise. The interstitial fluid velocity, not the superficial velocity (defined below), becomes the determinant of residence time in the vicinity of reaction sites. For steady flow in any arbitrary channel, the fluid velocity increases in places of reduced cross-sectional area (contractions) as noted previously. Porous media contain networks of small channels. The average interstitial fluid velocity due to the network of small channels in porous media is quantified through the porosity (ε). It is simply the fraction of the bulk volume which is made up of pores, i.e. the void fraction, which is also the fraction of a channel's cross-section open to flow. For a steady flow rate Q in a channel of cross-sectional area A, the average superficial velocity is

$$v_s = Q / A \tag{8}$$

The average interstitial velocity is

$$v_i = Q / (\epsilon A) = v_s / \epsilon \tag{9}$$

For uniformly sized spheres, the most efficient packing gives a porosity of approximately 26% (based on face-centered cubic or hexagonal close packing). Such highly ordered packing likely does not occur in a chromatography column. An arrangement known as random close packing is more probable. The porosity of a randomly close-packed bed of spheres is 36% based on numerical simulation[13]. Therefore in a column packed (randomly) with uniformly sized beads, the interstitial velocity is 2.8 as high as the superficial velocity. This is a best case scenario. For beads with a distribution of sizes, packing is more efficient and the porosity decreases which leads to even higher interstitial velocities when a constant flow rate is maintained.

There is an additional subtlety that arises in porous media. Equation (9) gives the interstitial velocity for a porous medium in which the pores completely span the medium and are parallel to the principle flow direction. However, since the pores in a packed column form zig-zag channels, the actual flow path is tortuous and therefore longer than the superficial length of the packed column. With this consideration, Equation (9) now gives the component of the interstitial velocity in the principal flow direction. Therefore, the fluid velocity magnitude must be higher along the true flow path to maintain a steady flow rate. It is sometimes assumed for rough calculations that the zig-zag path makes an angle of forty-five degrees with the superficial flow direction[10]. With this assumption, the interstitial

velocity becomes

$$v_i = \sqrt{2}\ v_s / \epsilon \qquad (10)$$

Thus, interstitial velocities in tightly packed porous media can be quite significant. This is depicted graphically in Figure 3. In addition to velocity changes due to contracting and expanding channels, fluid elements near the particle surfaces experience accelerations and decelerations around the irregular and curved contours. This can lead to local turbulence in flows through porous media characterized by low Reynolds numbers in the range 1-100[14,15].

The energy dissipation associated with fluid flow through porous media is

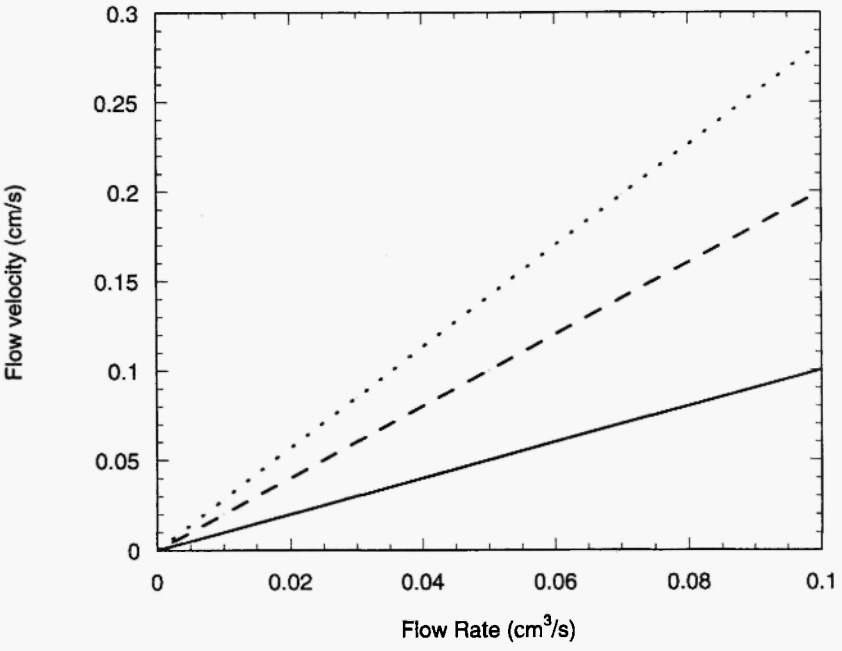

Fig. 3: Effect of porous media on average fluid velocities in non-turbulent flows through a closed channel with a cross-sectional area of 1 cm^2. (A) Solid line: Velocity-flow rate relationship in an unrestricted channel. (B) Dashed line: Flow through a 50% porous medium with pores which span the medium parallel to the direction of flow. (C) Dotted line: Estimated velocity in a 50% porous medium with zigzag channels as would be found in a bead-packed column.

greater than that for flow in a straight, open channel due to the higher pressures needed to maintain a given flow rate. Such considerations should be included in the design of miniaturized, low power (battery operated) sensors. The need for more pump work in a sensor based on porous media (compared to an unobstructed capillary channel) would require larger (capacity) energy storage devices to maintain sensor lifetime.

A column packed with beads yields a three-dimensional presentation of antibodies as well as three-dimensional flow patterns. Potentially, this situation can give rise to events which are detrimental to system sensitivity such as labeled-antigen recapture by free antibody binding sites. The dimensionality and the probability of rebinding are reduced by utilizing a membrane as the solid support matrix. If the membrane is thin, the presentation of capture antibodies is essentially planar, a two-dimensional situation. However, the dimensional character of the flow will depend on the porosity and pore type of the membrane. A highly porous membrane with pores that span its thickness will cause little deflection from the principle flow direction, and convection of material would occur in essentially one dimension. However, a low-porosity membrane may cause significant flow in directions perpendicular (radial) to the principle direction since streamlines will impinge on impermeable regions of the membrane. In this situation, flow patterns will be three-dimensional. Pores that do not span the membrane will also cause flow patterns to become multi-dimensional. An additional factor which may strongly influence the flow characteristics in a membrane-based sensor is the design of the chamber which houses the membrane.

Although the flow patterns in porous media are complex, the multidimensional fluid motion breaks up the laminar character of the flow (but does not necessarily cause turbulence). This allows flow in porous media to be treated as "plug" flow in which very little axial (flow direction) dispersion of an analyte occurs due to velocity differentials in the fluid [11]. This only applies to fluid within the porous media. Once the flow has left the reactor (and before it enters), a laminar profile will again develop (depending on the length and design of distal fluidics chambers). Since bead- and membrane-based sensors present a significant portion of the immobilized antibodies normal to the flow direction, convection is the dominant mass transport process which delivers analyte to detection sites.

KINETICS CONSIDERATIONS IN THE DISPLACEMENT IMMUNOSENSOR

The displacement kinetics of the fluorophore-labeled antigen from the immobilized antibody in the flow immunoassay are represented by the following reaction utilizing the law of mass action:

$$AbAg^{*} + Ag \rightleftharpoons AbAg + Ag^{*} \qquad (11)$$

where $AbAg^{*}$ is the complex of immobilized antibody and labeled antigen; Ag is the unlabeled antigen added during each sample injection; AbAg is the complex of immobilized antibody and unlabeled antigen; and Ag^{*} is the labeled antigen displaced from the antibody and detected downstream. It is important to distinguish between **continuous flow displacement** and **standard flow injection** configurations. Both assays are conducted under non-equilibrium, flow or pulse flow conditions. However, signal generation in standard flow injection assays relies exclusively on association kinetics (k_a), while signal generation in continuous flow displacement assays relies on dissociation kinetics (k_d) of the labeled-antigen in conjunction with association of the unlabeled antigen. Consistent with this, the performance of flow displacement assays improves with increasing k_d, while the performance of standard flow injection assays does not.

Other ongoing reactions in the flow immunosensor system are: the displacement of an unlabeled antigen by another unlabeled antigen; the displacement of labeled antigen by another previously displaced labeled antigen; and the displacement of unlabeled antigen by already displaced labeled antigen. The first two reactions have no net effect on sensitivity, while the latter would be detrimental to the function of a sensor. Depending on the solid support material, non-specific adsorption of labeled and unlabeled antigen to the solid surface could also adversely affect system performance.

A theoretical model to describe the displacement of bound labeled antigen from immobilized antibody under flow conditions has been formulated[4]. This model was developed using the continuous flow immunoassay employing monoclonal antibody covalently immobilized in a bead-packed column. Several factors known to influence antibody binding were investigated in detail including flow rate and antibody density. To investigate the effect of flow rate on the displacement kinetics, the undissociated fraction (θ) of labeled antigen at each step of the repetitive displacement can be calculated. It is calculated from the difference between total bound labeled antigen and the amount displaced after

each addition of unlabeled antigen using the following relation:

$$\theta(t) = \frac{[bound\ Ag^*]_{t=0} - \sum [displaced\ Ag^*]_t}{[bound\ Ag^*]_{t=0}} \quad (12)$$

The displacement efficiency (D_e) is described by the relationship:

$$D_e = \frac{[displaced\ Ag^*]}{[loaded\ Ag]} \quad \frac{1}{\theta} \quad (13)$$

where the [loaded Ag] was constant during the repetitive displacement experiments. The experimental data suggested that the displacement reaction could be suitably approximated by a first order rate process shown in Equation (14).

$$d\,[AbAg^*]/\,dt = -k_d\,[AbAg^*] \quad (14)$$

Thus the apparent dissociation constant (k_d) can be analyzed at various flow rates and antibody densities using the following equation:

$$k_d = -\frac{\ln\theta}{t} \quad (15)$$

where the time period available for displacement (t) is determined by dividing the volume of the column containing the immobilized antibody by the flow rate[4]. The term "apparent" dissociation reflects the fact that the constant is calculated from the amount of labeled antigen released from the column. This constant is a function not only of the actual k_d of the antibody but also of the antibody-independent factors such as nonspecific binding of labeled and unlabeled antigen molecules and accessibility of the antigen-binding sites.

DISSOCIATION KINETICS

In the displacement flow immunoassay, continuous dissociation of labeled antigen from the immobilized antibodies occurs even in the absence of competing unlabeled antigen. A concentration gradient of dissociated antigen between the liquid layer adjacent to the matrix surface and the bulk solution is created by the introduction of flow, thereby enhancing the transport of dissociated antigen away from the antibody binding sites[16]. This spontaneous dissociation creates unoccupied antibody binding sites which ultimately affects

the magnitude of the displacement signal generated.

To evaluate the impact of this phenomenon, the law of mass action can be extended to solid-phase binding assays. Rabbany *et al.*[16] analyzed the dissociation kinetics of labeled antigen under continuous flow conditions. Solution-phase kinetic equations were modified to account for immobilization of the antibody and to describe the dissociation kinetics at the solid-liquid interface. The dissociation patterns observed with different flow rates indicate that flow rate is directly correlated to the apparent dissociation rate constant. This is in accordance with an earlier report describing a decrease in the binding constant of antigen and immobilized antibody with increasing flow rates[17]. The effect of the flow on the dissociation kinetics was determined by calculation of the apparent dissociation rate constants (k_d) which increase with an increase in the flow rate. These dissociation rate constants are approximately 20- to 30-fold lower than those obtained from displacement studies (i.e., in the presence of competing unlabeled antigen). The difference in the dissociation rate constants obtained in the two studies is most likely a function of the greater degree of reassociation of labeled-antigen in the absence of unlabeled-antigen[16].

ADDITIONAL KINETICS CONSIDERATIONS

Immobilization of antibody on a solid support alters the kinetics of the antibody-antigen interaction, exemplifying how variations in a single physical parameter can drastically alter the behavior of the biomolecule[18]. Several kinetic differences are apparent between free versus immobilized antibody[19] In addition to potential mass transport limitations, other variables introduced by immobilization may include heterogeneity in antibody affinity, difference in relative affinity for labeled versus unlabeled antigen, and antibody density.

A theoretical treatment of heterogeneity in the context of a displacement reaction at equilibrium was recently given[20]. The theoretical results indicated that equilibrium isotherms for displacement reactions are less sensitive to affinity distributions than are isotherms for typical association/dissociation reactions. For a system using monoclonal antibodies, heterogeneity is expected to be minimal. However, heterogeneity may be induced upon immobilization to a solid support. This possibility was investigated by applying the heterogeneity theory to data from a flow displacement assay for TNT[21]. To apply the theory, it was assumed that the flow rates were low enough to allow a quasi-equilibrium state to be reached. The results indicated that any heterogeneity introduced via the covalent

immobilization techniques was essentially undetectable.

A variety of additional factors influence the recognition function of the antibody-antigen complex at the solid-liquid interface[22 23]. The chemistry of the detection event is mediated by the interaction of the analyte nonspecifically with the surface itself and with the solvent. Many organic substances have limited solubility in water and readily adsorb to hydrophobic surfaces such as plastics. Accordingly, surfactant or dilute organic solvents may be necessary. These could potentially denature the antibodies to an extent that affects their antigen binding characteristics. The availability of the secondary reactants in the sample may also affect signal generation (cross-reactivity). Temperature changes, extremes in pH, and proteolytic degradation can destroy either the functional biomolecule or the analyte, resulting in signal reduction. Thus, the antibody molecule is only one of many elements that affect recognition and signal transduction. Characterization of these parameters will enable design of a flow immunoassay with maximum detection sensitivity.

FLOW DISPLACEMENT IMMUNOASSAY PERFORMANCE

A. Bead Assay

Flow-displacement immunoassays were initially developed using columns containing immobilized antibodies on porous beads[7], which maximize surface area in the compact micro-columns. One antigen/antibody system which was extensively investigated was cocaine/anti-cocaine. A monoclonal antibody specific for both cocaine and its major metabolite, benzoylecgonine, was immobilized onto beads and saturated with Texas Red cadaverine-labeled antigen. Aliquots of this detection matrix were dispensed into small, disposable columns and buffer solution was pumped through to remove unbound fluorophore-labeled antigen. The column eluent was monitored using a fluerometer. Samples containing various concentrations of cocaine diluted in buffer were introduced into the flow stream after a suitable baseline had been established. Figure 4 shows an actual trace resulting from the repetitive displacement of labeled benzoylecgonine by repeated injections of a concentrated cocaine sample. Figure 5 demonstrates the application of the kinetic analysis given previously to this data.

The effect of flow rate on the displacement kinetics of the labeled antigen is shown in Figure 6A. Samples of cocaine were injected repeatedly at flow rates of 0.5, 0.75, and 1.0 mL/min into 200 μL columns containing immobilized

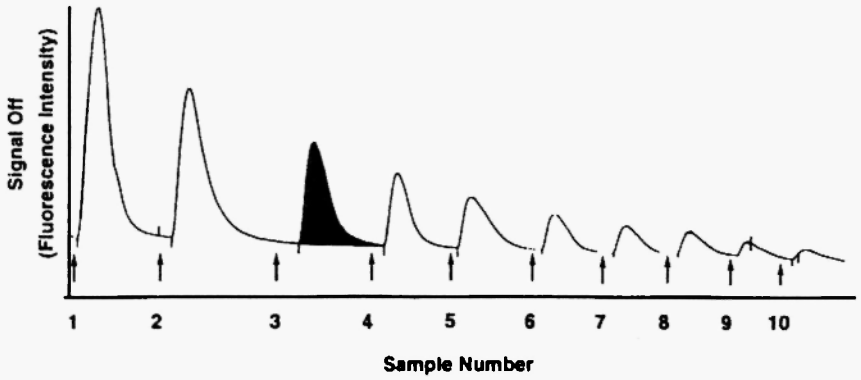

Fig. 4: Actual signal generated by the repetitive displacement of fluorescein-labeled benzoylecgonine utilizing the flow immunoassay at a flow rate of 1 mL/min. The plot illustrates the column depletion which occurs upon repeated injections of highly concentrated analyte solutions. The concentration was the same for all injections in this case. Total peak areas as shown by the shaded example are used for quantitative analysis.

anti-cocaine antibody. The amount of labeled-antigen displaced increased with decreasing flow rates since the analyte was provided more time to interact with the immobilized complex. This results in an inverse relationship between the displacement efficiency previously described and flow rate[4,18]. Apparent dissociation constants (kd) were found to be proportional to the flow rate. A two-fold increase in flow rate resulted in a two-fold increase in apparent dissociation constants. This trend was independent of antibody density.

The effect of antibody density on the kinetics and detection sensitivity of a solid-phase displacement immunoassay was investigated[6]. Increasing the density of immobilized antibodies, and hence the concentration of antibody-bound labeled antigen, should enhance the probability of the unlabeled antigen displacing the labeled antigen. This should increase the *detection sensitivity* since the rate of displacement is proportional to the density of antibody-bound labeled antigen. Figure 6B illustrates the labeled-antigen released from the matrices coated with different densities of antibodies.

Comparison of a high and low antibody matrix density revealed that the high density matrix was the more sensitive (based on the fluorescence signal above

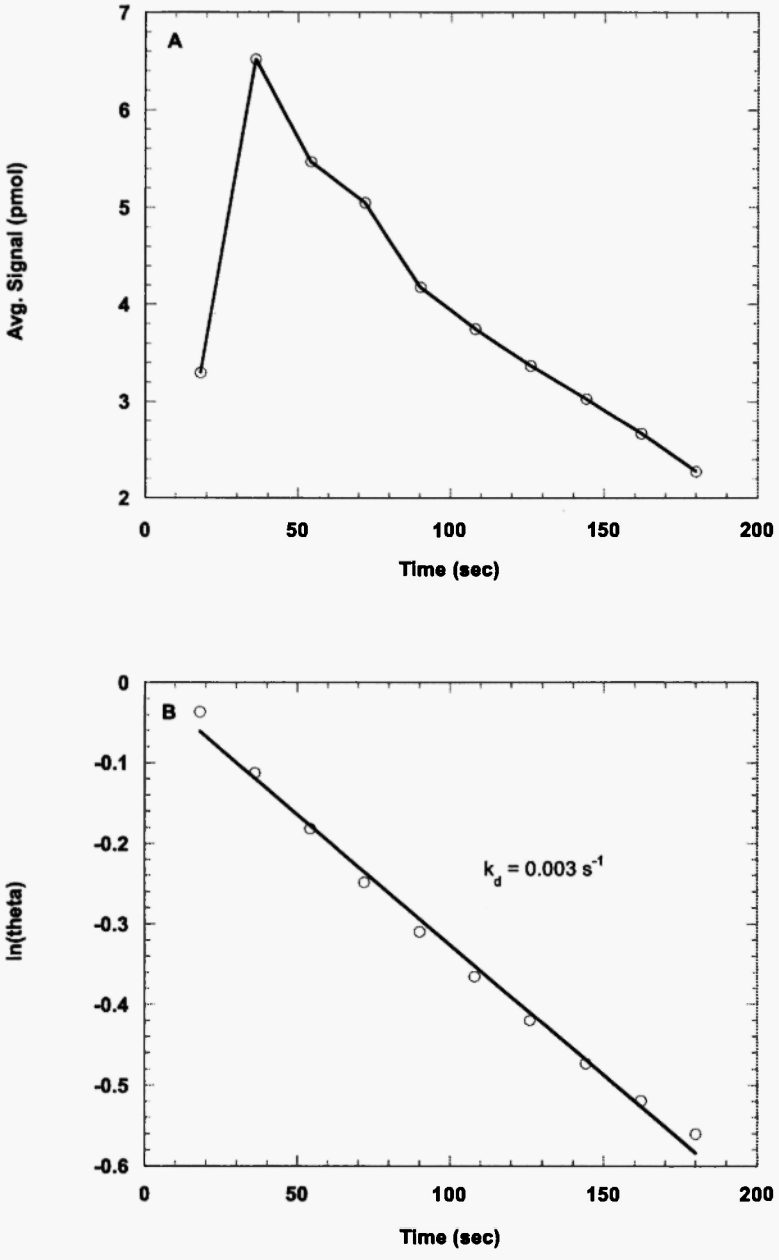

Fig. 5 (cont'd):

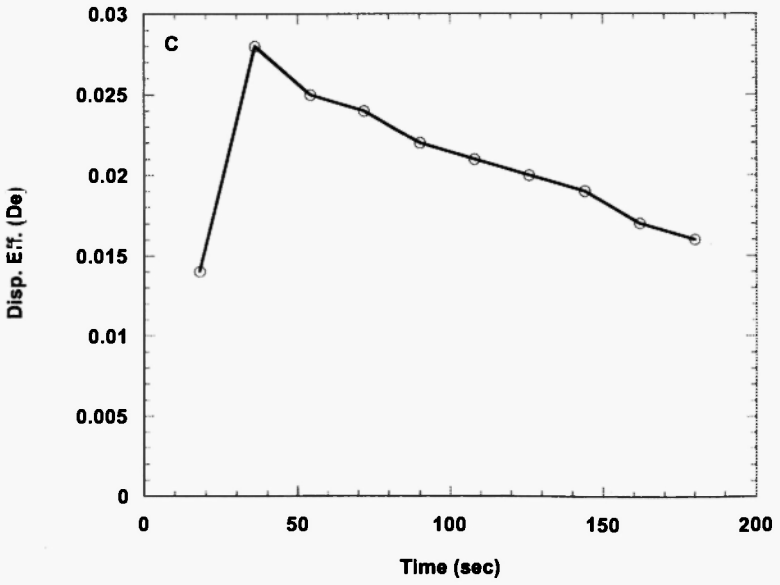

Fig. 5: Kinetic analysis of the data presented in Figure 2. (A) Juxtaposition of the signal responses from individual injections yields a curve which approximates the behavior which would be obtained from a continuous infusion of analyte. (B) The decrease in the fraction of bound labeled antigen calculated from the curve in (A). The slope gives the apparent dissociation constant k_d. (C) The displacement efficiency as a function of time. The increase between the first two injections is attributed to free antibody binding sites.

baseline). The detection sensitivity is a function of at least two parameters, the density of antibody-bound labeled antigen and the density of unoccupied antibody binding sites. Unoccupied antibody binding sites are generated by spontaneous dissociation of bound labeled antigen under flow conditions. These unoccupied binding sites could interfere with the sensitivity of the flow immunoassay since they are capable of binding to unlabeled antigen, thus reducing the amount of unlabeled antigen able to displace labeled antigen. Furthermore, rebinding to displaced labeled antigen may reduce the fluorophore-generated signal. A higher density of antibody will provide a higher amount of bound labeled antigen, while concurrently generating a greater density of unoccupied binding sites. For the high density matrix, these unoccupied

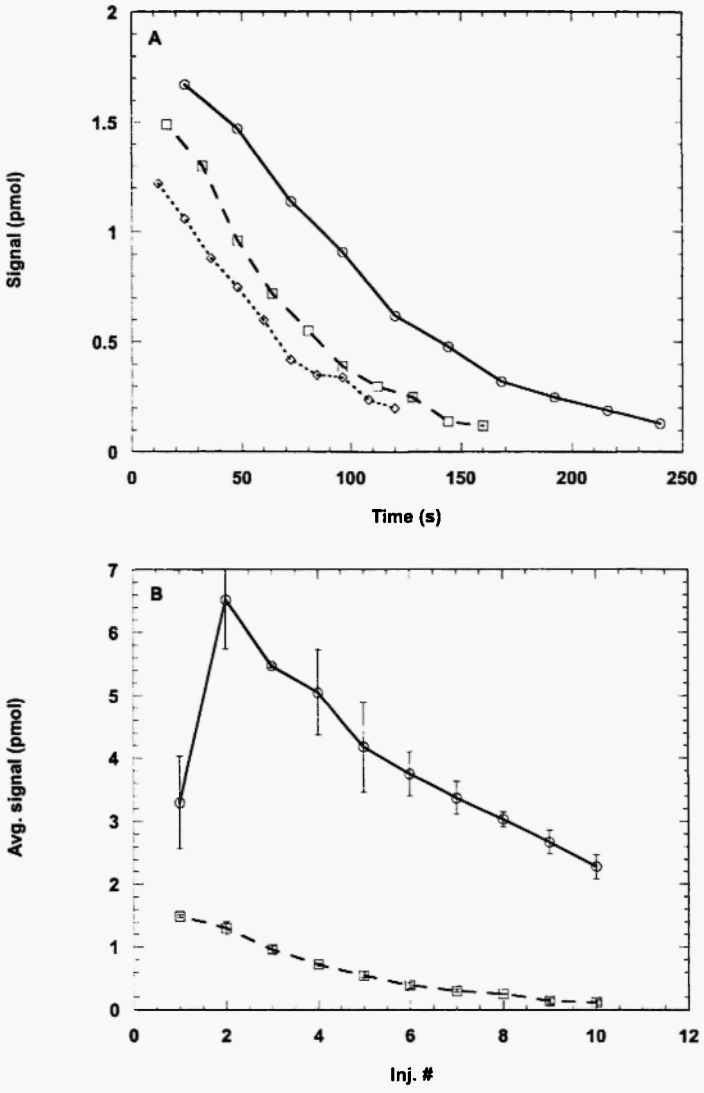

Fig. 6: (A) The effect of flow rate on the displacement of labeled antigen. Solid line: 0.5 mL/min. Dashed line: 0.75 mL/min. Dotted line: 1.0 mL/min. The data represent the mean of two experiments. The displacement efficiency decreases with increasing flow rates, but the displacement rate increases with the flow rate. (B) Labeled antigen displacement from high density (solid line, 245 pmol of immobilized antibody) and low (broken line, 50 pmol of immobilized antibody) density matrices. Samples of cocaine were injected repeatedly at a flow rate of 0.75 mL/min. The data represent the mean ±S.E. of two experiments.

binding sites decreased the *detection sensitivity* for the first sample injected but not for the subsequent samples. However, the signal from the first injection was higher than that from the low density column. The kinetics analysis presented previously indicates that the higher antibody density is associated with a lower apparent dissociation constant[6].

Several problems are inherent in the bead-based assay. The beads are difficult to load into the column in exact quantities, and the quantity of beads in the column has a direct effect on the magnitude of the signal generated. A smaller number of beads reduces the probability that an unlabeled antigen molecule will encounter and displace a labeled antigen from the antibody, thereby reducing the signal magnitude. Flow stream tunneling (continual changes of flow pathways due to packing rearrangements) may lead to more efficient packing of the matrix over time. This may reduce the surface area over which the injected analyte can interact with the immobilized complex and thus the signal magnitude generated.

B. Membrane Assay

A membrane-based system solves problems associated with the bead-based assay since it possesses a stable two-dimensional geometry with negligible height. The advantages include facility and reproducibility of immobilizing the antibody, simpler insertion of the membranes into the reaction chamber, and more reproducible mass transfer characteristics for the displacement reaction. In addition, the flow apparatus can be miniaturized for easier storage and reduced cost when a membrane replaces the beads as the matrix support for antibody immobilization.

Another low molecular weight hapten, 2,4,6-trinitrotoluene (TNT), was detected with the membrane-based flow immunoassay. Monoclonal antibodies with a specificity for TNT were immobilized on porous membranes consisting of a nylon mesh which was modified to incorporate unspecified (proprietary) surface reactive sites that facilitated the covalent binding of proteins. Membranes were cut into circular disks and were incubated in anti-TNT solutions varying in concentration. After immobilizing the antibody, the unreacted sites were blocked following the protocol described previously[24]. The membranes were then dispensed into a small disposable flow-through column containing a frit (thin, porous glass plug) at its base with a 100 µL head volume. The membrane was secured in place by using the barrel of a 1 mL plastic syringe, cut to the proper height. The available antibody binding sites were saturated with

fluorophore-labeled antigen solution and incubated at room temperature overnight. The particular sulfoindocyanine dye (Cy 5) used for the analyte labeling was used because of its superior physical properties, such as solubility, high quantum yield, and spectral characteristics[25].

The membrane was tested in a laboratory flow system consisting of a peristaltic pump and a fluorescence detector. A buffer solution containing ethanol to ensure solubility of the TNT was pumped through the flow system in order to remove nonspecifically-bound fluorophore-labeled antigen. The experiments were run at flow rates ranging from 0.25 to 2.0 mL/min. When the background fluorescence stabilized, samples of analyte diluted with the buffer solution were injected into the flow. A typical dose-response curve is shown in Figure 7. The membrane-based immunosensor for TNT (as currently operated) has a limit of detection in the high pg/mL concentration range.

Characterization of the effects of flow rate and antibody concentration on the performance of the membrane-based detection system yielded similar results to

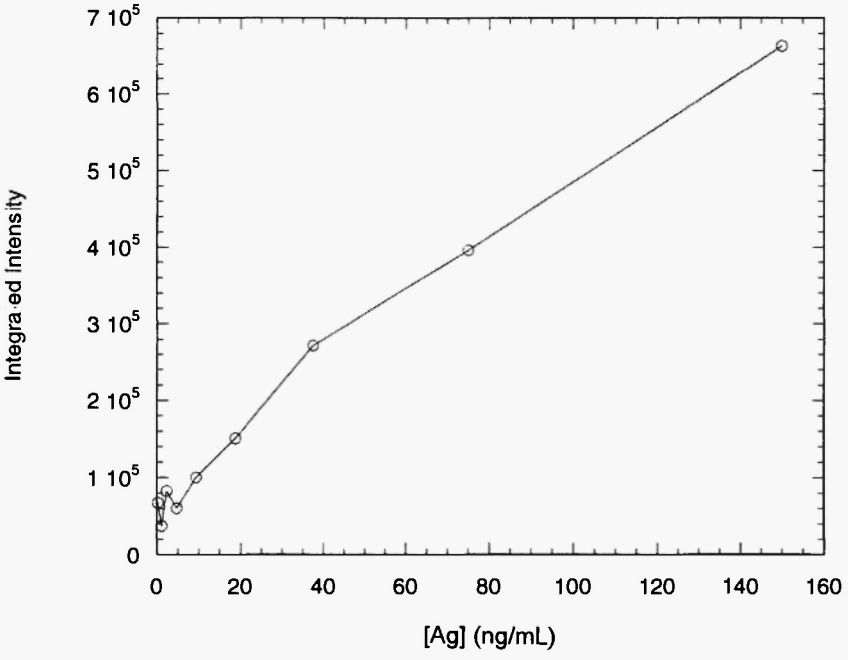

Fig. 7: Dose-response curve illustrating the integrated areas of peaks obtained from 100 µL injections of TNT solutions into a membrane based immunosensor. The flow rate was 0.5 mL/min.

those from the bead-based assays[18]. The inverse relationship between signal response and flow rate holds true for the membrane configuration. And, as with the bead-packed columns, a high antibody density gives a higher displacement signal than does a low density, but the displacement efficiency is reduced compared to that of the low density membranes.

C. Capillary Assay

Antibodies against TNT or RDX were immobilized in borosilicate glass capillaries 550-800 μm in diameter using a silane-based chemistry[9]. The immobilized antibodies were incubated with labeled antigen as done with the bead and membrane-based systems. With a length of 20 cm and a flow rate of 250 μL/min, a capillary-based sensor for TNT increased the sensitivity (limit of detection 15 pg/mL or 7 fmol) by two orders of magnitude over the existing packed-column and membrane-based systems[9]. This was accompanied by a short response time (3 min) after injection, which represents a 20-fold decrease in assay time when compared to standard analytical techniques such as HPLC and GC/MS. A dose-response curve demonstrating sensitivity to TNT in the low pg/mL range and a dynamic range spanning five orders of magnitude is shown in Figure 8.

The TNT displacement efficiencies of the capillary sensor used in this initial work and of an optimally configured packed column sensor were 25% and 0.11%, respectively. This superior performance was initially (and incorrectly) attributed to a higher surface area to volume ratio. However, a quick calculation shows that the capillary geometry offers the smallest surface area to volume ratio of the three solid supports. Therefore, the underlying fluid dynamic and mass transport phenomena, as well as a host of other physical and chemical variables, require further scrutiny if comparative performance evaluations are to be made between the packed-column, membrane, and capillary flow sensor configurations.

In a second study of capillary-based sensors[26], the responses of two different TNT antibodies were compared along with the effects of varying two physical parameters of the system: flow rate and capillary length. The results of the comparison of the two different TNT antibodies provided confirmation of the attribution of cross-reactivity to specific antibody function. The influences of flow rate and capillary length were in qualitative agreement with the theoretical considerations presented previously: longer column length and/or lower flow rate increase the sensitivity of the system. The limit of detection of TNT was

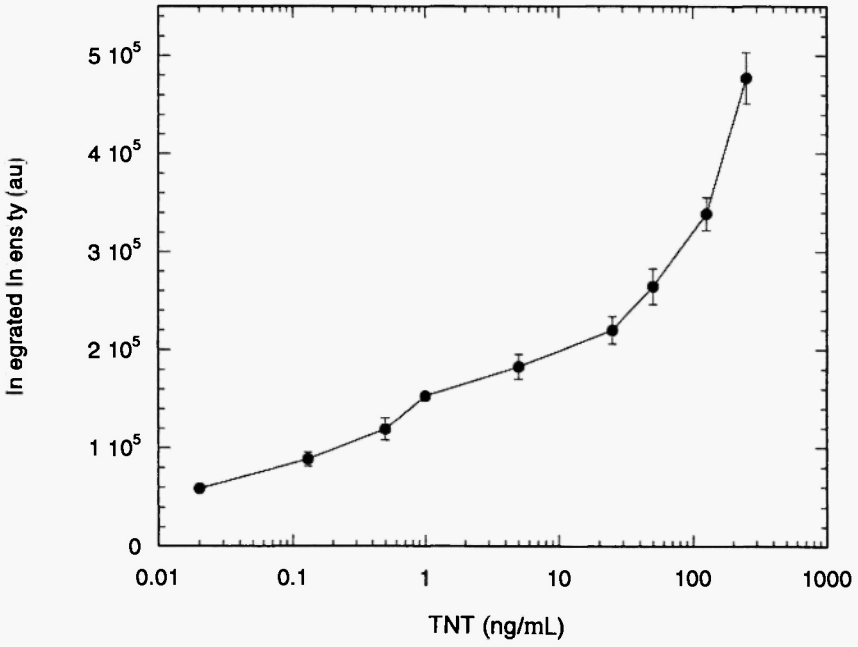

Fig. 8: Dose-response curve from a capillary-based immunosensor for TNT. 100 μL injections were made in triplicate. The data shown are the mean ±S.E.

decreased from that attained in the first study to 1 pg/mL (0.44 fmol) by lowering the flow rate to 50 μL/min.

To expand the capability of displacement assays to multi-analyte detection, a capillary multi-analyte system was configured by connecting two capillaries, one containing anti-TNT and the other anti-RDX, to a flow splitter[27]. This format was successful at detecting mixed, aqueous samples of TNT and RDX. The limits of detection at a flow rate of 100 mL/min (through each capillary) for TNT and RDX were 100 and 500 pg/mL, respectively. This loss of sensitivity (compared to individually run capillaries) was attributed to dilution effects from the additional tubing and splitter required to build the multi-analyte sensor. Cross-reactivity of the anti-TNT capillary for RDX and vice-versa was minimal.

D. Discussion

The three solid supports, beads, membranes, and capillaries, have proven to be effective matrices for the construction of displacement immunosensors. As

a spectrum of advantages and disadvantages are presented by each, the choice of which to use must be based on the demands of a given application. For routine field testing, portability, ease of handling, and repetitive use are important criteria. Membranes are well suited to such activity, and a portable, membrane-based immunosensor has been field tested and is now commercially available. When greater sensitivity is required, a capillary-based system would be a better choice based on currently available data.

The origin of the superior sensitivity of the capillary-based immunosensors over those built around bead-packed columns or membranes remains to be determined. Calculations using the experimental parameters show, for instance, that average interstitial fluid velocities in the bead-based system are just as slow or slower than those encountered in the capillaries. This, combined with the tortuous flow path, ensures that analyte is in the vicinity of antibodies for a comparable (if not longer) amount of time in the porous medium as in the capillary sensor. Therefore, it is not a simple factor of residence time. As previously indicated, the surface area to volume ratio is lower in the capillary than for the other two solid supports, and the antibody surface density is known to be lower in the silica capillaries than in bead-packed columns and on the polyamide membranes. Thus, these parameters also fail to provide an explanation. Additional factors include the influence of the specific support material (silica or polymer) on the kinetics and affinity of the antibody-antigen interactions, and the volume of analyte solution injected relative to the reactor volume. Computer simulations are currently underway to investigate and optimize these parameters for displacement immunosensors based upon the three different solid supports.

APPLICATIONS

Antibody-based detection methods have become widely accepted for medical diagnostics and on-site environmental monitoring[28, 29]. Immunosensors show great promise for automating such diagnostic procedures with possible increases in the speed and/or sensitivity of the analysis. However, several limitations have up to now restricted wide acceptance. For environmental monitoring, cost is a major consideration. Immunosensors must compete with test kits based on modified ELISA systems and the frequency of use must be high enough to justify the cost of the instrument[30]. For medical diagnostics, serial analysis as performed in an immunosensor makes such systems more suitable for doctor's office and

bedside use than in large hospital laboratories which require high throughput clinical analyzers. For the doctor's office cost and frequency of use again become major considerations. For aviation security, immunosensors can provide appropriate sensitivity and accuracy, but analysis time and the requirement for sampling into water are significant issues. Immunosensors are well suited for on-site testing for drugs of abuse since quantitation and accuracy are particularly important. There is also a clear advantage in being able to retest a subject immediately rather than after a lag due to sending a sample to a central laboratory. Monitoring of manufacturing processes and food/water safety are also areas where immunosensors may make an important contribution. Unlike the flow immunosensor, the majority of immunosensors described in the refereed literature have not been automated for repetitive use by non-technically trained operators, nor have many demonstrated reliable operation outside a laboratory environment.

Flow displacement immunosensors have been tested in widely varied applications. These include the detection of explosives for aviation security[31,32], pollution remediation[33], detection of polychlorinated biphenyls in groundwater[34], detection of drugs of abuse in urine and saliva[35], detection of cortisol in clinical fluids[36,37], detection of pesticides[38] and the detection of antibiotics in milk (A. Kusterbeck, unpublished data). Assays for detection of hormones in seawater which may affect coral reef survival and for detection of PAHs in groundwater are currently under development.

Several instruments for conducting displacement assays in flow are being developed. LifePoint, Inc (Rancho Cucamonga, CA) is developing a handheld device for analysis of drugs in saliva. Research International has commercialized a membrane-based flow immunosensor, the FAST 2000 (Flow Assay Sensing and Testing) which is the size of a portable CD player and plugs into the PCMCIA port of a laptop computer for on-site data analysis and archival. And the Naval Research Laboratory is developing a chip-based system for the capillary immunosensor with multianalyte detection capability.

CONCLUSION

This review has focused upon the development and application of flow displacement immunosensors. Broader reviews of immunosensor technology may be found in Rabbany *et al.*[39] and Ghindilis *et al.*[40] Flow displacement sensors have several advantages over other immunosensor methods for the

detection of small molecules. First, displacement assays are faster (1-3 min) than most competitive or sandwich immunoassays (5-30 min). Second, there are no washing or reagent addition steps to add to the complexity of an automated fluidics system. Third, the device required to perform the displacement assays is very simple and relatively inexpensive, basically requiring only a pump, light source and photo-detector. Fourth, a single antibody-coated membrane can be used repeatedly so that reagent use is minimized. Fifth, the displacement assay has proven to be accurate, quantitative, and sensitive to ppb levels of a variety of analytes in most non-opaque, aqueous samples. Finally, it has been used extensively outside the laboratory and has been successfully operated by users previously unfamiliar with the technology.

Several limitations of displacement assay design remain in developing a reliable sensor system. Issues to be addressed include calibration procedures, effect of fouling on the sensor substrate and fluidics control. Current quantitation procedures require a direct comparison of sample fluorescence intensities (integrated areas) to a calibration standard. As discussed with bead assays, the depletion of the fluorescence with repeated injections will eventually compromise absolute quantitation, though positive or negative samples may still be recognized (see Figure 4). Also, complex sample matrices such as seawater or opaque fluids, may affect fluorescence measurements by causing non-specific release or masking of the fluorescent molecules, respectively. Finally, since flow characteristics are critical to assay performance, an understanding of the interplay of the underlying fluid dynamics with the chemical kinetics and diffusional processes are needed to design optimized sensors. In application, this requires accurate and precise fluidics control, a task which becomes increasingly difficult as sensor sizes become smaller and smaller. Though such issues remain to be addressed in the optimization and application of flow displacement immunosensors, the technology holds great promise for the future of biochemical sensing techniques.

REFERENCES

1. Vo-Dinh, T., Tromberg, B.J., Griffin, G.D., Ambrose, K.R., Sepaniak, M.J., and Gerdenshire, E.M., *Appl. Spectrosc.* **41**, 735 (1987).
2. Yalow, R.S., and Berson, S.A. *Nature* **184**, 1648 (1959).
3. Ligler, F.S., Gaber, B.P., Kusterbeck, A.W., and Wemhoff, G.A. US Patent No. **5,183,740** (1993).

4. Wemhoff, G. A., Rabbany, S.Y., Kusterbeck, A.W., Ogert, R.A.,Bredehorst, R., and Ligler, F.S. *J. Immunol. Meth.* **156**, 223 (1992).
5. Ligler, F.S., and Rabbany, S.Y., in: *Synthetic Microstructures in Biological Research*, ed. by Schnur, J.M., and Peckerar, M., Plenum Press, New York,1992, p. 67.
6. Rabbany, S. Y., Kusterbeck, A. W., Bredehorst, R., and Ligler, F. S. *J. Immunol. Meth.* **168**, 227 (1994).
7. Kusterbeck, A.W., Wemhoff, G.A., Charles, P.T., Yeager, D.A., Bredehorst, R., Vogel, C., and Ligler, F.S. *J. Imunnol. Meth.* **135**, 191 (1990).
8. Rabbany, S.Y., Pritsiolas, L.M., Marganski, W.A., Kusterbeck, A.W., and Ligler, F.S. Membrane-based Displacement Immunoassay, 18th IEEE Engineering in Medicine and Biology Conference, Amsterdam, The Netherlands, 1996.
9. Narang, U., Gauger, P. R., and Ligler F. S. *Anal. Chem.* **69**, 1961 (1997).
10. DeNevers, N. *Fluid Mechanics for Chemical Engineers*, 2nd ed., McGraw-Hill, Inc., New York, 1991.
11. Ruzicka, J., and Hansen, E.H. *Flow Injection Analysis*, John Wiley & Sons, New York, 1981, pp. 31-50.
12. Oran, E.S., and Boris, J.P. *Numerical Simulation of Reactive Flow*, Elsevier, New York, 1987, p. 32.
13. Jaeger, H.M. and Nagel, S.R. *Science* **255**, 1523 (1992).
14. Giddings, J.C. *Dynamics of Chromatography- Part I. Principles and Theory*, Marcel Dekker, Inc., New York, 1965, p. 218.
15. Richter, P., Ruiz, B.L., Sanchez-Cabezudo, M., and Mottola, H.A. *Anal. Chem.* **68**, 1701 (1996).
16. Rabbany, S.Y., Piervincenzi, R.T., Kusterbeck, A.W., Bredehorst, R., and Ligler, F.S. *Analytical Letters* **31**, 1663 (1998).
17. Sportsman, J.R., and Wilson, G.S. *Anal. Chem.* **52**, 2013 (1980).
18. Rabbany, S. Y., Kusterbeck, A.W., Bredehorst, R., and Ligler, F.S. *Sensors and Actuators B* **29**, 72 (1995).
19. Mason, D.W., and Williams, A.O. *Biochem. J.* **187**, 1 (1980).
20. Selinger, J.V., and Rabbany, S.Y. *Anal. Chem.* **69**, 170 (1997).
21. Rabbany, S. Y., Piervincenzi, R., Judd, L., Kusterbeck, A. W., Bredehorst, R., Hakansson, K., and Ligler, F. S. *Anal. Chem*, **69**, 175 (1997).
22. Nygren, H., Werthen, M., and Stenberg, M. *J. Immunol. Methods* **101**, 63 (1987).

23. Stenberg, M., and Nygren, H. *J. Theor. Biol.* **113**, 589 (1985).
24. Rabbany, S.Y., Marganski, W.A., Kusterbeck, A.W., Ligler, F.S. *Biosensors and Bioelectronics* **13**, 939 (1998).
25. Bart, J.C., Judd, L.J., Hoffman, K.E., Wilkins, A.M., Charles, P.T., and Kusterbeck, A.W. *Development and Applications of Immunoassays for Environmental Analysis*; ACS Symposium Series, American Chemical Society: Washington, DC (1996).
26. Narang, U., Gauger, P. R., and Ligler F. S. *Anal. Chem.* **69**, 2779 (1997).
27. Narang, U., Gauger, P. R., Kusterbeck, A.W., and Ligler F. S. *Anal. Biochem.* **255**, 13 (1998).
28. Van Emon, J.M., & Lopez-Avila, V. *Anal. Chem.* **64**, 79A (1992).
29. Gerdes, M., Meusel, M., and Spener, F. *Anal. Biochem.* **252**, 198 (1997).
30. Crockett, A.B., Craig, H.D., Jenkins, T.F., and Sisk, W.E. EPA Federal Facilities Forum, EPA/540/R-97/501 (1996).
31. Warden B.A., Allam K., Sentissi A., Cecchini D.J., and Giese R.W. *Anal. Biochem.* **162**, 363 (1987).
32. Whelan, J.P., Kusterbeck, A.W., Wemhoff, G.A., Bredehorst, R., and Ligler, F.S. *Anal. Chem.* **65**, 3561 (1993).
33. Bart, J.C., Judd, L.L., Hoffman, K.E., Wilkins, A.M., and Kusterbeck, A.W. *Environ Sci. Technol.* **31**, 1505 (1997).
34. Charles P.T., Conrad D.W., Jacobs M.S., Bart J.C., and Kusterbeck A.W. *Bioconjugate Chemistry* **6**, 691 (1995).
35. Parsons, R.G., Kowal, R., LeBlond, D., Yue, V.T., Neagarder, L., Bond, L., Garcia, D., Slater, D., and Rogers, P. *Clinical Chemistry*, **39**, 1899 (1993).
36. Kaptein, W.A., Zwaagstra, J.J., Venema, K., Ruiters, M.H.J., and Korf, J. *Sensors and Actuators B* **45**, 63 (1997).
37. Kronkvist, K., Lövgren, U., Svenson, J., Edholm, L., and Johansson, G. *J. Immunol. Methods* **200**, 145 (1997).
38. Lehotay, S.J., Wright, S.F., DeMilo, A.B., and Stanker, L.H. 21st Annual Federation of Analytical Chemistry and Spectroscopy Societies Conference, St. Louis, MO 1994.
39. Rabbany, S.Y., Donner, B.L., and Ligler, F.S. *Crit. Rev. Biom. Eng.* **22**, 307 (1994).
40. Ghindilis, A.L., Atanasov, P., Wilkins, M., and Wilkins, E. *Biosensors & Bioelectronics* **13**, 113 (1998).